HHS Public Access

Author manuscript

Neuropsychologia. Author manuscript; available in PMC 2020 April 01.

Published in final edited form as:

Neuropsychologia. 2019 April ; 127: 158–170. doi:10.1016/j.neuropsychologia.2019.03.001.

Posterior parietal influences on visual network specialization during development: an fMRI study of functional connectivity in children ages 9 to 12

Jonathan F. O'Rawe, **Anna S. Huang**, **Daniel N. Klein**, and **Hoi-Chung Leung**

Department of Psychology, Stony Brook University

Abstract

Visual processing in the primate brain is highly organized along the ventral visual pathway, although it is still unclear how categorical selectivity emerges in this system. While many theories have attempted to explain the pattern of visual specialization within the ventral occipital and temporal areas, the biased connectivity hypothesis provides a framework which postulates extrinsic connectivity as a potential mechanism in shaping the development of category selectivity. As the posterior parietal cortex plays a central role in visual attention, we examined whether the pattern of parietal connectivity with the face and scene processing regions is closely linked with the functional properties of these two visually selective networks in a cohort of 60 children ages 9 to 12. Functionally localized face and scene selective regions were used in deriving each visual network's resting-state functional connectivity. The children's face and scene processing networks appeared to show a weak network segregation during resting state, which was confirmed when compared to that of a group of gender and handedness matched adults. Parietal regions of these children showed differential connectivity with the face and scene networks, and the extent of this differential parietal-visual connectivity predicted individual differences in the degree of segregation between the two visual networks, which in turn predicted individual differences in visual perception performance. Finally, the pattern of parietal connectivity with the face processing network also predicted the foci of face-related activation in the right fusiform gyrus across children. These findings provide evidence that extrinsic connectivity with regions such as the posterior parietal cortex may have important implications in the development of specialized visual processing networks.

Corresponding Author: Hoi-Chung Leung, Stony Brook University, Department of Psychology, Stony Brook, N.Y., 11794-2500, hoi-chung.leung@stonybrook.edu.

Author Contributions

H-C.L and D.K. developed the experimental design and study protocol. A.H. collected data and contributed to experimental design. J.F.O. developed analysis approach, conducted analyses, and together with H-C.L prepared the manuscript.

Conflict of Interest Statement

None of the authors have any conflicts of interest.

Data Accessibility

Access to supporting data and materials are available upon request from the corresponding author.

Keywords

posterior parietal cortex; visual specialization; development; face processing network; scene processing network

1. Introduction

The visual system is known to be topographically organized in the primate brain, with increases in both complexity of stimulus selectivity and size of receptive field moving downstream along the ventral visual pathway (Mishkin & Ungerleider, 1982; Van Essen & Gallant, 1994). Functional specialization of visual areas has been observed for many complex object categories, such as faces, scenes, objects, word forms, and number forms (Cohen et al., 2000; Epstein & Kanwisher, 1998; Kanwisher, McDermott, & Chun, 1997; Shum et al., 2013). For simplicity, our discussion focuses on the face processing network. Though most study results were generated by comparing face and scene processing networks, some general principles are likely shared across other object domains at the network level. The nature of face specialization in the visual cortex and how it develops has been a matter of debate over a period of decades (see Grill-Spector, Weiner, Kay, & Gomez, 2017 for full review). To extend the previous studies of local mechanisms, we examined a potential extrinsic mechanism on the emergence of visual processing networks in children ages 9–12.

1.1 Local mechanisms in visual selectivity and topography

Previous studies have found distinguishable local or regional structural and functional properties between visual areas. Four different cytoarchitectonic regions were defined in the fusiform gyrus (FG1–4) in postmortem human brains (Caspers et al., 2013; Lorenz et al., 2017). These specialized cellular architectures are thought to provide the basis for particular computations in the inferotemporal regions which result in specialized responses to objects and faces. A recent study combining fMRI and cytoarchitectonic approaches further suggested that not only does the PPA have distinct cytoarchitecture from the FFA, the two distinct clusters of the FFA in the fusiform gyrus (pFus/FFA-1 and mFus/FFA-2) are separable in accordance with the cytoarcitectually defined subregions (FG1–4) (Weiner et al., 2017). Due to the limitation of the postmortem study approach, a direct link between regionally specific cellular architecture and face selective activation has yet to be established.

Nonetheless, neuroimaging measures of local variations in cellular composition and in conjunction with BOLD signal selectivity have provided supporting results. For instance, local structural properties such as decreased T1 relaxation, increased local fractional anisotropy, decreased mean diffusivity, and lower cortical thickness were found to be related to more selective BOLD responses in the inferotemporal cortex and better performance in face perception (Gomez et al., 2017, 2015; McGugin, Van Gulick, & Gauthier, 2016).

Exactly what computations the local architecture is allowing for is currently unclear or unspecified by most models. A recent set of neuroimaging studies modeling receptive field

properties provides a potential clue. Using the population receptive field (pRF) method, it was shown that the FFA receptive field properties are both less eccentric and larger than earlier visual regions, which may reflect a potential outcome of integration across the features of the face (Kay, Weiner, & Grill-Spector, 2015). A computational model of feedforward integration of features onto a complex face filter (e.g. a prototype) demonstrated a relatively good fit to the BOLD responses in face specialized regions in the infertemporal cortex (Kay & Yeatman, 2017). It's been theorized, on the basis of this type of computation, that particular topography emerges along the inferotemporal cortex due to the competition for representational resources with regard to receptive fields (Behrmann & Plaut, 2013; Malach, Levy, & Hasson, 2002).

1.2 Extrinsic mechanisms in visual selectivity and topography

Beyond the local biases of visual processing, the anatomy of the visual system also suggest that extrinsic connectivity can shape visual selectivity (Kravitz, Saleem, Baker, Ungerleider, & Mishkin, 2013). Extrinsic mechanisms may explain certain results that are puzzling if only local properties are considered. For one, the receptive fields in the inferotemporal change in size and eccentricity on the basis of task demand (Kay et al., 2015). Such dynamic effects are more likely resulting from some extrinsic influence, rather than local processing constraints. Indeed, the feedforward model of BOLD responses in the ventral pathway showed an increased fit when considering extrinsic connectivity from the posterior parietal cortex (Kay & Yeatman, 2017). Further, visual specialization has been demonstrated for object categories of very similar demand of visual resources, such as the word form and number form areas (Cohen et al., 2000; Shum et al., 2013). The role of extrinsic connectivity in visual organization has been proposed multiple times throughout the literature (Hannagan, Amedi, Cohen, Dehaene-Lambertz, & Dehaene, 2015; Johnson, 2011; Kravitz et al., 2013; Palmeri, Wong, & Gauthier, 2004). It was postulated that a region or a set of regions may develop a particular functional specialization because of the constraint of the pattern of their anatomical connectivity with the rest of the brain. This has been referred to as the "Biased Connectivity Hypothesis" to address the differential emergence of the visual word form area and the number form area (Hannagan et al., 2015).

One way for extrinsic connectivity to provide information regarding behaviorally relevant stimulus qualities is through enhancing certain features of the attended object (Goldstone, 2003). Such extrinsic connectivity would afford the ventral visual regions to gain stimulus selectivity above and beyond what would be predicted by the feedforward models alone, indicated by evidence demonstrating that lower order features do not fully explain activity patterns in categorically selective visual association regions (Proklova, Kaiser, & Peelen, 2016). A direct demonstration of visual representation shift from feature to categorical was found in the monkey lateral intraparietal area (LIP) across learning, with a high fidelity sensory signal at early learning that shifts into a categorical signal as a decision task was learned (Sarma, Masse, Wang, & Freedman, 2016). While it is unclear how and to what extent extrinsic connectivity contributes to the specific topographic layout of functional specialization, there is some preliminary evidence that extrinsic connectivity patterns (including the posterior parietal) can predict the spatial topography of visually selective

regions in the inferotemporal cortex during development (Osher et al., 2016; Saygin et al., 2016).

1.4 Posterior Parietal Cortex as a possible extrinsic mechanism in shaping selective visual processing

In this study, we focused on the potential roles of posterior parietal connectivity on visual specialization in children, as it is well recognized that the posterior parietal cortex plays an important role in both spatial and object attention (Buschman & Miller, 2007; Egly, Driver, & Rafal, 1994; Silver, 2005). Its close anatomical connections with both the inferotemporal and frontal regions put the posterior parietal cortex in a unique position for modulating visual processing and action planning (Blatt, Andersen, & Stoner, 1990; Kravitz, Saleem, Baker, & Mishkin, 2011; Seltzer & Pandya, 1984). There is some evidence of differential anatomical connectivity along the parietal lobe to different visual processing regions in nonhuman primates, along the infereotemporal cortex and within the thalamus (Cavada & Goldman-Rakic, 1989; Schmahmann & Pandya, 1990; Seltzer & Pandya, 1984). While the exact homology between monkey and human parietal cortices is contested (Culham & Kanwisher, 2001; Husain & Nachev, 2007; Orban, 2016; Orban, Van Essen, & Vanduffel, 2004), human neuroimaging studies have demonstrated a parcellation in the posterior parietal cortex resembles that of the nonhuman primates. For instance, both human angular gyrus and monkey area 7a show dense connections with parahippocampal gyrus, both human supramarginal gyrus and monkey area 7b show dense connections with supplementary motor cortex, and both the human superior parietal lobule/intraparietal sulcus (SPL/IPS) and monkey area LIP show dense connections with the superior colliculus (Rushworth, Behrens, & Johansen-Berg, 2006). Both monkey areas 7a (tentative human AG), and monkey area LIP (tentative human SPL/IPS) demonstrate connections to both parahippocampal gyrus and across the inferotemporal cortex (Blatt et al., 1990; Seltzer & Pandya, 1984), providing the potential to modulate responses along categorically selective cortex in the inferotemporal cortex.

Mounting evidence supports that the posterior parietal cortex plays a particular role in transforming high fidelity stimulus representation to representations that can direct action, from action oriented object representation (Shmuelof & Zohary, 2005) to reward driven stimulus categorization during learning (Sarma et al., 2015). Such top-down processes have been implicated in theoretical models of visual specialization (Goldstone, 2003). The primary role of posterior parietal cortex indeed has been suggested to be top-down control of visual processing and memory (Dolan et al. 1997; Eger et al. 2007). Intriguingly, category selective responses to visual stimuli have been consistently observed for LIP neurons (Janssen, Srivastava, Ombelet, & Orban, 2008; Sereno & Maunsell, 1998; Swaminathan & Freedman, 2012) and reported for posterior parietal regions in humans (Konen & Kastner, 2008; Vuilleumier, Henson, Driver, & Dolan, 2002). Hence, some suggested that it is the connectivity between the dorsal and ventral visual areas that give rise to integrated object representation in the brain and this representation is used for action planning (Helbig, Graf, & Kiefer, 2006; Singh-Curry & Husain, 2009).

1.5 Visual specialization and parietal maturation during childhood

Visual specialization shows multiple trajectories across development. Global topology of the inferotemporal cortex seems to be intact at a young age (Golarai, Liberman, & Grill-Spector, 2017; Golarai, Liberman, Yoon, & Grill-Spector, 2010), as young as 3–8 months old (Deen et al., 2017), which may reflect more fundamental organizations, such as animacy/inanimacy (Kriegeskorte et al., 2008). However, the degree of selectivity, the size of the selective clusters, and the stability of location of the face processing network develop from childhood through adolescence (Deen et al., 2017; Golarai et al., 2017, 2010; Scherf, Behrmann, Humphreys, & Luna, 2007). Indeed, while visual experience seems necessary for the development of face selective cortex (Arcaro, Schade, Vincent, Ponce, & Livingstone, 2017), this does not seem to be the case for animacy/inanimacy categorization in the inferotemporal cortex (Mahon, Anzellotti, Schwarzbach, Zampini, & Caramazza, 2009; Mahon & Caramazza, 2011).

In particular, fMRI studies of early adolescents also revealed weak or no suprathreshold activation at the group level for faces in the inferotemporal cortex in comparison to that of young adults (Aylward et al., 2005; Scherf et al., 2007). The precise developmental timecourses of these networks are hard to determine as most previous studies are cross sectional. Nonetheless, largescale systematic analyses of event-related potential (ERP) data in response to face perception have identified two periods of accelerated development, ages 8–11 and 14–15 (Taylor, Batty, & Itier, 2004).

Interestingly, the earlier period of development of ERP signals corresponds with the age range just prior to which fMRI studies find stable enough topology across children to produce significant adult-like clusters at the group level (Aylward et al., 2005; Golarai et al., 2007; Scherf et al., 2007). Across these studies, both size and intensity of fusiform gyrus activation predicts the variance in performance in face recognition tasks across children (Golarai et al., 2007; Scherf et al., 2007). Scene specific topology, on the other hand, seems to have a much less protracted development, with children 5–8 years old potentially already demonstrating adult like patterns in the right parahippocampal gyrus (Golarai et al., 2007; Scherf et al., 2007).

At the same time, the parietal lobe is going through significant development. More specifically, the maturation of the lateral parietal cortex shows a spatial gradient, superior/medial to inferior/lateral, with the lateral parietal regions reaching peak grey matter volume around 8.5 years and superior/medial regions at an earlier age (Giedd et al., 1999; Gogtay et al., 2004). A similar pattern was replicated in a more recent study of surface area of the parietal cortex (Jernigan, Brown, Bartsch, & Dale, 2016). These findings on the developmental gradient of the posterior parietal cortex, along with its close anatomical connections with inferotemporal cortex, put it in the critical position to contribute to the specialization of visual processing networks in children. We therefore used it as a good first candidate for testing the biased connectivity hypothesis.

1.6 Present study: posterior parietal cortex and visual specialization in children

In this study, we examined whether and how the pattern of posterior parietal functional connectivity with the visual networks is related to the functional properties of categorically selective networks in the ventral visual pathway in mid to late childhood. FMRI data were acquired from a group of children ages 9 to 12, a potential age range in which face selectivity starts to stabilize with the coincidental development of the parietal lobe, while they performed a visual stimulus matching task and during resting state (with no explicit task). We expected to find differential functional connectivity between the superior/medial and inferior/lateral parietal areas and the face and scene processing networks in these children. We further tested whether children's network distance between the face and scene network, which seems to differ from an adult sample, is related to their connectivity with the posterior parietal cortex. Lastly, we explored whether the spatial location of the right FFA is dependent on the pattern parietal-face network connectivity in the same group of children. Our results suggest that a stable connectivity pattern between posterior parietal cortex and inferotemporal visual processing regions stabilizes their functional location and network properties, supporting the biased connectivity hypothesis in this group of children.

2. Methods

We utilized a face and house identity matching task to functionally localize face and scene selective regions of interest. We then examined the resting state network properties of these face and scene regions in these children as well as a group of adults for comparison. To address the main question on the relationship between parietal connectivity and visual network organization, we examined whether the organization of the face and scene networks varies by their connectivity strength with particular parcels of the parietal lobe, and to what extent this relationship can explain the observed age group differences in face and scene network organization. To further specify the function of parietal connectivity, we tested the extent to which the pattern of parietal connectivity can predict individual differences in the spatial location of the rFFA, which is a very specific prediction from the "Biased Connectivity Hypothesis".

2.1 Subjects

We collected behavioral and fMRI data from a community sample of 80 children. These children were a subsample of the 559 children enrolled in the Stony Brook Temperament Study (see Olino, Klein, Dyson, Rose, & Durbin, 2010). They were recruited from the community through commercial mailing lists, were screened for any major medical conditions, and were required to have at least one English speaking biological parent. After exclusion based on excessive motion artifacts in either the resting state or task state scans (< 2/3 of data remaining), a total of 60 participants (29 Female), ages 9–12 (M = 10.23, SD = 0.95) remained in the final fMRI data analysis. Due to computer error, usable behavioral data from the stimulus identity matching task were retained for only 43 participants; thus only these individuals were included in the behavioral data analysis and across-subject correlations between fMRI measures and task performance. Informed consent was obtained from the parental guardians of the children in accordance to the Stony Brook University Institutional Review Board.

For comparison purposes in the network segregation analysis, we utilized the resting-state fMRI data of a gender and handedness matched group of 60 adults from the Cambridge Buckner subset of the 1000 Connectomes Project (Biswal et al., 2010) with an attempt to match the age variance of our child sample, ages 20–23 (M = 21.17, SD = 0.96) (See Table S1 for a detailed list of subjects).

2.2 General and fMRI Procedures

On the day of scanning, prior to any data collection, each child was acclimated to the scanning environment in a mock scanning session (MRI simulator of Model number: PST-100355, Psychological Software Tools, USA). During both the mock and the actual scanning procedure, foam pads were used to reduce head movement.

During fMRI, we first collected the resting state data over two sessions (each ~6 minutes) separated by a structural acquisition. Participants were instructed to keep their gaze at the center of three concentric circles, so the condition was the same as mock scanning. Afterwards, the participants performed the stimulus identity matching task during fMRI (see below).

2.3 Stimulus Identity Matching Task during fMRI

Each child participant performed three iterations of four types of task blocks that lasted 16 seconds each in one of the two pseudo-random orders (Fig. 1A). These task blocks were interleaved with 14-sec of fixation. The four different block conditions were defined by the stimulus type: neutral faces, sad faces, happy faces, and houses. At the beginning of each block, there was a one second warning period, in which the fixation cross changed in color from black to blue cuing the starting of the block, followed by four trials (two match trials and two non-match trials). Each trial began with a fixation cross that lasted 600 ms followed by the simultaneous presentation of two images for 3000 ms, in which participants made a button press to indicate whether the two images were identical or different. To assure compliance we monitored the participants' eye position utilizing an Eyelink 1000 eye-tracking system (SR Research Ltd., Mississauga, ON, Canada). Data from this task were previously reported in an earlier paper from our group (Kann, O'Rawe, Huang, Klein, & Leung, 2017).

2.4 Image Data Acquisition

All images from the children involved in this study were acquired in a Siemens Trio 3 T scanner. For each child, high resolution structural images were acquired using the following MPRAGE sequence: slices = 176, TR = 2400 ms, TE = 3.16 ms, flip angle = 8°, matrix size = 256 × 256, FOV = 256 × 256 mm, voxel resolution = 1 × 1 × 1 mm^3. Afterwards, inplane T2-weighted structural images were collected in the axial-oblique plane, aligned to the AC-PC with the following parameters: slices = 37, TR = 6450 ms, TE = 88 ms, flip angle = 120°, matrix size = 256 × 256, FOV = 256 × 256, voxel resolution = 1 × 1 × 3.5 mm^3. During both resting and task-state sessions, T2*-weighted axial-oblique images, in the same orientation of the inplane images, were acquired using the EPI sequence with the following parameters: slices = 37 (interleaved), TR = 2000 ms, TE = 30 ms, flip angle = 90°, matrix size = 64 × 64, FOV = 224×224 mm, resolution = 3.5 × 3.5 × 3.5 mm^3. All children

completed two resting state sessions with a total of ~11.7 minutes of data collected (350 volumes) and a total of ~6.2 minutes of task data (186 volumes).

The adult image data from the Cambridge Buckner sample included: T1-weighted structural images (MPRAGE: slices = 192, matrix size = 144 × 192, resolution = 1.20 × 1.00 × 1.33 mm^3) and resting-state functional images (EPI: 47 interleaved axial slices, TR = 3000 ms, resolution = 3.0 × 3.0 × 3.0 mm^3, about 6 minutes of data with 119 volumes).

2.5 Image Preprocessing

Images were preprocessed with SPM8 (http://www.fil.ion.ucl.ac.uk/spm8/) and CONN (http://www.alfnie.com/software/conn). Prior to analysis, images were slice time corrected, realigned to the temporally middle volume according to a 6 parameter rigid body transformation. Structural images were coregistered with the mean functional image, segmented, and then normalized to a standard space utilizing the MNI template using both linear and nonlinear transformations. Functional images were then normalized utilizing the same parameters as the structural normalization. Finally, the images were smoothed to a 6 mm FWHM Gaussian kernel.

For functional connectivity analysis of the resting state data, additional preprocessing steps were performed. A nuisance regression was constructed to regress out the following confounding variables: 6 motion parameters up to their second derivatives, scans with excessive motion (Euclidean Norm > 0.5 || Global Signal (z) > 3.0), effects of block onset, modeled physiological signal generated through aCompCor of the white matter and CSF voxels, and the linear drift. The residuals from this nuisance regression were then filtered utilizing a bandpass between the frequencies of 0.008 and 0.09 Hz and despiked. We chose not to regress out the global signal in order to retain the interpretability of negative correlations (Murphy, Birn, Handwerker, Jones, & Bandettini, 2009). That is, negative correlations should represent a true inverse relationship between regions.

2.6 General Linear Model for task data and ROI selection

With the task data, a General Linear Model (GLM) was constructed using SPM8 (https://www.fil.ion.ucl.ac.uk/spm/software/spm8/). Each stimulus condition was modelled in the GLM as a regressor using a boxcar function convolved with the canonical hemodynamic response function. The 6 motion parameters and volumes with high motion (Euclidean Norm > 0.5 || Global Signal (z) > 3.0) were entered into the model as covariates of no interest. Beta values were estimated for each voxel for each condition. The estimated parameters of this model were utilized to generate the contrasts of interest (face vs. scene) which were then used for ROI selection.

Functional regions of interest (ROIs) of face and scene related regions were defined using two approaches. First, the children's second level face vs scene contrasts were used. Spherical ROIs of a 5-mm radius (volume = 19 voxels) around the peak coordinates of activation clusters at the group level within several canonical regions in the face and scene networks. All the face and scene related regions were identified at $p < .001$. Second, a set of unbiased ROIs were defined using Neurosynth meta-analyses (Yarkoni, Poldrack, Nichols, Van Essen, & Wager, 2011), with the exception of the anterior temporal face patch (ATFP)

which was chosen from a separate meta-analysis (Von Der Heide, Skipper, & Olson, 2013), as the ATFP was not revealed in the Neurosynth meta-analysis. Functional network connectivity analyses were conducted using each set of ROIs. All results were qualitatively replicated across the two sets of ROIs. Thus, we reported results from the ROIs defined using our stimulus matching task as the focus of this study is on the children.

To study how parietal connectivity contributes to the variance in functional location of the rFFA, we further selected the ROIs for each individual subject using an automated procedure. First, to generate a large search volume, layers of voxels were added to the initial group FFA cluster (from the Face > House contrast as described above), until it reached at least 400 voxels. This accreted version of the group cluster served as the search volume for each individual child participant. For each individual, the top 30% of voxels within the 400 voxel search volume were selected followed by outlier removal. The remaining clusters were weighted based on a linear combination of the following factors: closeness to group coordinate, average beta value for cluster, and cluster size. The cluster with the highest z-score was selected, and then a sphere was drawn around its centroid coordinate. This procedure, in comparison to selecting top 10% or top 20% of voxels, or picking peak coordinates instead of the centroid, produced a tighter ROI probabilistic distribution, and increased the overall correlation between contralateral homologs (i.e.. rFFA and lFAA) (Fig S1).

Five posterior parietal parcels were defined in each hemisphere using the Automated Anatomical Labeling atlas (AAL) (Tzourio-Mazoyer et al., 2002), including the left and right: angular gyrus (AG), supramarginal gyrus (SMG), precuneus (PCu), inferior and superior parietal lobules (IPL and SPL) (Fig. S2). We selected all available posterior parietal parcels within the AAL atlas for the anatomical driven approach to examine differential connectivity of parietal areas with the two visual selective networks.

2.7 Resting-State Functional Connectivity: ROI-based and voxel-based analyses

Time series correlation analyses were applied to the preprocessed resting-state fMRI data (see above). For each subject, the mean cleaned time courses were extracted from each ROI within the face and scene networks and the posterior parietal cortex. Next, the mean signals from the ROIs were correlated with each other generating a k x k order correlation matrix for each subject where k is the number of ROIs. Each element of this matrix was then transformed using Fisher's Z transformation to make them amenable to group analysis. Prior to any quantifications, each subject's Fisher's Z matrix were split into positive and negative connectivity matrices. The negative connectivity matrices were absolute valued to ensure symmetric computations.

We first calculated several summary measures to quantify the relationships within and between networks for the face and scene networks in the children (and the adult sample for reference). To quantify the within network strength for each subject, we averaged all the Fisher's Z values between each of the unique bivariate relationships within a network (Fig. 1B, black arrows). This measure provides a metric for the strength of the intrinsic connectivity of a predefined network (i.e. how much it is acting like a network). Analogously, between network connectivity was quantified by averaging the connections

between two networks. This provides a metric that was used to quantify the distance between two networks. The distance between two networks, or network segregation, can be thought of as the a network marker for the specialization of networks (Rubinov & Sporns, 2010).

We then quantified the connectivity strength that an extrinsic ROI (i.e. parietal areas) has with the face and scene networks for each subject, by averaging all the Fisher's Z values between the extrinsic ROI and each node of the network (Fig 1B, red arrows). For each extrinsic ROI, the ROI to face/scene network connectivity strength values were averaged across the two hemispheres to produce a single index for that particular ROI. Finally, we utilized the correlation between these two measures, extrinsic ROI-network connectivity and intrinsic network connectivity, as a benchmark index of the influence of an extrinsic ROI has on the face/scene network (Fig. 1B, right table). For example, if the extent to which a certain parietal ROI connects to the face network predicts the face network's intrinsic network connectivity strength, we would say that the extent to which the face network is acting like a coherent network is dependent on that parietal ROI's connectivity. We utilized the five AAL parietal parcels described above to explore for parietal influences on intrinsic network connectivity in the face and scene networks. To correct for the multiple analyses for modulatory effects, we set FWE = .05 given the 5 independent sets of statistical tests. However, our results remain consistent even when correcting more conservatively for each correlation (2 per region, 10 tests in total).

We also repeated the extrinsic connectivity analyses to the whole brain. The same metrics described above were applied to each to the voxel, generating voxel-wise network correlation maps (the extent to which every voxel in the brain correlates on average with each network) as well as voxel-wise maps of the correlations between the network correlation at each voxel and each network's intrinsic network connectivity strength. This was to confirm that our ROI results replicate at the voxel level, as the parietal parcels are large and likely functionally heterogeneous to some extent. We also used the whole brain face network correlation maps from this analysis to examine the relationship between patterns of parietal connectivity with the face network and the spatial location of the rFFA in individual subjects.

2.8 Correlation between spatial location of rFFA and parietal connectivity

In accordance with the predictions of the biased connectivity hypothesis we further tested if the spatial location of the functionally defined rFFA would depend on parietal connectivity. We performed a partial least squares (PLS) regression, a technique which maximizes the covariance between two multivariate sets of data. We extracted the top two components from a PLS regression of the parietal portion of the voxel-face network connectivity strength maps, from the whole brain connectivity maps described above (section 2.7), in predicting the location of each subject's rFFA centroid (x, y, z). The parietal-visual network connectivity patterns were then visualized by plotting them in a two dimensional heat map collapsing across the D-V dimension and then characterized by their correlation to the ROI-Network correlation strength measures. Participants were then split into two groups for each component based on positive and negative PLS scores; then each subject's centroid location

was plotted, color coded by low or high PLS score. This latter step provided further visualization and quantification on how different functional connectivity patterns between the parietal cortex and the face network constrain the location of the functionally defined rFFA.

3. Results

3.1 Behavioral results, and face and scene related activations

Behavioral responses of the children during the stimulus matching task were less accurate at face matching (M = 0.75, SD = 0.20) than house matching (M = 0.88, SD = 0.11), $t(42) = -6.23$, $p < .001$ (Fig. 1C), though the average response time between face (M = 1418.47 ms, SD = 206.92 ms) and scene (M = 1371.90 ms, SD = 231.73 ms) conditions were more comparable, $t(42) = 1.99$, $p = 0.053$. A closer examination of the distributions revealed that the children's accuracy on face trials exhibited a bimodal distribution, though this performance heterogeneity was not driven by a particular face condition as the bimodal distribution was observed for each condition (Fig. 1C).

The children's fMRI data from the stimulus matching task revealed a subset of the typical nodes of the face processing network, including the bilateral FFA, bilateral superior temporal sulcus (STS), and bilateral anterior temporal face patch (ATFP) in the face > scene contrast (Fig 1D, see Table 1 for list of coordinates and Supplemental Table 2 for full list of suprathreshold clusters). Among these face related activations, only STS and ATFP in the right hemisphere the reached cluster level significance threshold in the group contrast map (FDR corrected $p < .05$), suggesting a relatively weak or variable face processing network in these children shown in the previous literature (Aylward et al., 2005; Scherf et al., 2007). (Note: The spatial distribution of activation patterns was similar among the three face conditions; data not shown). In addition, since we observed bimodality of the behavioral data, the sample was separated by performance using a median split, and a two-sample t-test was used to confirm that the high and the low performers showed similar activation patterns.

Using the house > face contrast, the typical nodes of the scene processing network were identified in these children. Significant activation clusters were found in bilateral transverse occipital sulci (TOS), retrosplenial cortices (RSC), and parahippocampal gyri (PPA) (FDR < 0.05; see Fig. 1D and Table 1 for list of coordinates and Table S2 for a list of all suprathreshold clusters).

3.2 Strength of functional connectivity within and between Face and Scene networks during resting state Fmri

We examined the resting-state Fmri functional connectivity patterns of the face and scene networks in the children and adult samples using the ROIs defined in the child sample's group contrasts (Table 1). While there were little to no differences in within network connectivity between the child and adult samples in either the intrinsic face or scene network ($p's > .25$), differences emerged in the relationship between these two networks (Fig. 2). In comparison to the adults, the two visual networks showed a lower between-network negative connectivity in the children, $t(118) = -3.54$, $p < .001$ but a comparable between-network

positive connectivity pattern, t(118) = −1.80, p = .07, suggesting that these visual networks are less segregated in children. Qualitatively similar results were obtained when utilizing meta-analytic ROIs, with the primary difference between adults and children being between-network negative connectivity. We then wanted to examine whether this putative developmental difference in the face and scene processing networks, decreased distance in children, can be explained by extrinsic parietal connectivity. To do so, we first sought to identify regions of the posterior parietal cortex that differentially influence each of the processing networks in the children. Then we examined whether this differential influence could explain the network distances in the children.

3.3 Differential posterior parietal functional connectivity with face and scene networks

We quantified the relationship between the 5 different parcels of the posterior parietal lobule and the face and scene processing networks in children. Three out of the 5 parcels, Pcu, AG, and SPL, accounted for a significant amount of variance in the intrinsic connectivity of the face and scene processing networks of children (see Fig. S3A for Pcu, IPL, and SMG data).

The Pcu connectivity showed a significant correlation with the intrinsic connectivity of both visual networks, predicting the strength of intrinsic face network connectivity (r = 0.48, $p_{FWE} < .001$) and the intrinsic scene network connectivity strength (r = 0.78, $p_{FWE} < .001$). Nevertheless, the Pcu demonstrated a quantitative bias towards the scene network (z = −2.71, $p_{FWE} < .05$) (Fig. S3B).

The AG showed a significantly stronger relationship with the face network than the scene network (z = 3.73, $p_{FWE} < .001$), with AG-network connectivity strength significantly predicting the intrinsic face network connectivity strength (r = 0.62, $p_{FWE} < .001$) but not the scene network (r = 0.03, $p_{FWE} = 1.00$) (Fig. 3A, left).

In contrast, the SPL demonstrated a stronger relationship with the scene network, with the SPL-Scene network connectivity strength strongly predicting the scene network intrinsic connectivity (r = 0.60, $p_{FWE} < .001$). The SPL-Face network connectivity strength contributed only a modest proportion of the variance in the intrinsic face network connectivity (r = 0.30, $p_{FWE} = .09$). This difference was not significant after correction for multiple comparisons (z = −2.01, $p_{FWE} = .11$), but was when the outliers (determined by Cook's d) were removed (z = −3.04, $p_{FWE} < .01$) (Fig. 3A, right).

3.4 Parietal-visual network connectivity, visual network distance, and behavioral performance

We further examined to what extent the AG and SPL connectivity may account for the reduced network distance between the face and scene networks in these children (see Fig. 2C). Multiple regression analyses revealed that the parietal-visual functional connectivity significantly predicted face-scene network distance, for both positive and negative between-network connectivity, F(4,55) = 7.63, p < .001 and F(4,55) = 4.72, p < .001, respectively (Table 2). In particular, visual network's connectivity with the "non-preferential" parietal areas predicted a reduction in network distance of the two visual networks; that is, greater SPL-Face network connectivity strength was associated with stronger positive between-network connectivity (b = 0.327, p< .001) and weaker negative between-network

connectivity (b = −0.148, p < .05; Fig. 3B right) of the face and scene networks. The AG-Scene network connectivity effects followed a similar pattern (b = 0.122, p = 0.14; b = −0.122, p < .05; Fig. 3B left). In contrast, greater "preferred" AG-Face network connectivity strength was associated with stronger negative connectivity between the face and scene networks (b = 0.095, p < .05).

Furthermore, face-scene network distance predicted performance on both the face and house trials. Greater positive connectivity between the face and scene networks predicted poorer performance on both face (r = −.37, p < .05) and house trials (r = −.34, p < .05) (Fig. 4A, 4B). Further, greater negative connectivity between the two visual networks predicted better performance on house trials (r = .30, p < .05) (Fig. 4C). While the correlation between negative between-network connectivity and the children's performance on face trials did not reach statistical significance (r = .20, p = .20), it was numerically in the same direction.

Taken together, the AG and SPL demonstrated both a qualitative and quantitative difference in their influence on the visual network's intrinsic connectivity, showing preferential parietal influences on the face and scene processing networks, with AG showing preferential influence over the face processing network and the SPL showing preferential influence over the scene processing network. This differential influence accounted for a significant amount of variance in the distances between the face and scene processing networks, the putative developmental difference identified earlier.

3.5 Voxel-wise replication of the relationship between parietal connectivity on the face and scene network's intrinsic connectivity strength

To confirm that the differential effect of parietal connectivity on the intrinsic connectivity of the face and scene networks were not an artifact of averaging time-series within the large parietal parcels, we replicated the results using individually-defined face/scene ROIs in a voxel-by-voxel whole brain analysis. First we calculated the average connectivity between each node in the two visual networks and every voxel in the rest of the brain (Fig. 5A). Then, analogous to the analysis in Figure 3A, for each voxel, for each voxel, we calculated the correlation between the strength of voxel-visual network connectivity and the strength of intrinsic network connectivity for each visual network across subjects. Figure 5A displays the voxels that show a significant correlation between voxel-visual network connectivity and positive intrinsic network connectivity for the face network (red) and the scene network (blue). The spatial distribution of the differential parietal effect is consistent with the seed-based analysis. When quantifying the parietal connectivity effect by averaging across the voxels within the AAL parcels, the largest difference in the effect of parietal connectivity on face network and scene network connectivity again can be seen in AG and SPL, respectively (Fig. 5B).

3.6 Predicting rFFA location from parietal connectivity: PLS Regression

As previous studies have suggested that the face selective regions shift in location with development (Scherf et al., 2007), here we tested the possibility that the parietal connectivity with the face network may shape the location of the rFFA. We used a PLS regression to predict the spatial coordinates of each subject's rFFA activation centroid from their pattern

of parietal-face network connectivity (Fig. 6A). The first two components extracted from this analysis accounted for 24.92% of the variance in parietal-face network connectivity, and 31.26% of the variance in rFFA location.

More specifically, the Component 1 PLS scores were closely associated with intrinsic face network connectivity ($r = 0.53$, $p < .001$), suggesting again that parietal connectivity is important for maintaining connectivity within the face network (Fig. 6B). While Component 1 scores were positively correlated with all parietal ROI-face network connectivity strengths (p_{FWE}'s $< .05$), the AG-face network connectivity showed the strongest effect ($r = 0.79$, $p_{FWE} < .001$) (Fig 6C, top). Component 2 scores, however, only significantly positively correlated with SMG-face network connectivity strength ($r = 0.36$, $p_{FWE} < .05$) (Fig 6C, bottom).

Examining participants with high and low component scores allows us to parse out the corresponding effects of parietal connectivity on rFFA location. Splitting participants based on whether they had a positive or negative score on each of the component yielded the following groups High Component 1 (n = 30), Low Component 1 (n = 30), High Component 2 (n = 37), and Low Component 2 (n = 23). We compared their rFFA centroid locations, and found that those in the High Component 1 group showed a more posterior and ventral rFFA centroid location than the Low Component 1 group, $t(58) = -2.00$, $p < .05$, $t(58) = -3.92$, $p < .001$, respectively (Fig 6C, Bottom Right). Those within the High Component 2 group also showed a more posterior rFFA location, $t(58) = -2.64$, $p < .05$ (Fig 6C, Bottom Right).

4. Discussion

To study the role of extrinsic parietal connectivity in the emergence of functional specialization in the ventral visual cortex during late childhood or early adolescence, we analyzed the relationship between face/scene network's pattern of connectivity with the various posterior parietal regions. We then examined how this connectivity pattern related to the degree of intrinsic network connectivity within and network segregation between the two visual networks in a group of children ages 9 to 12. Our findings suggest that the lower negative connectivity between the two visual networks (i.e. less segregation) was closely linked with their differential connectivity with angular gyrus and superior parietal lobule, and that the children's performance on the visual discrimination task was associated with the degree of visual network distance. These findings map well onto the developmental time course in the extant literature (Gogtay et al., 2004; Scherf et al., 2007). In a more direct support for the biased connectivity hypothesis, our data revealed that the variation in the functional location of the rFFA can be predicted by the parietal-visual network connectivity patterns.

4.1 Role of the posterior parietal cortex in selective visual processing

Our findings suggest that the posterior parietal areas' differentially connectivity with the face and scene processing networks may have implications for the development of their specialization. There are several possible reasons why the parietal lobe may be important for the development of specialization. Given the parietal lobe's anatomical connections between both frontal and visual cortices, it's in a unique position to integrate sensory information and

task goal (Kravitz et al., 2011). Transformations of spatial information into many reference frames (e.g. eye-centered to head-centered to body-centered) within the parietal lobule provides a hint that one of the main parietal computations is perhaps for the purpose of preparing stimulus related information to be acted upon (Avillac, Denève, Olivier, Pouget, & Duhamel, 2005; Xing & Andersen, 2000). Indeed, through learning, representation of stimulus direction in the LIP neurons transforms from a state that is consistent with the incoming sensory information to a form that is consistent with the task goal (Sarma, Masse, Wang, & Freedman, 2015). This type of representation would be optimal for guiding the organization and development of visual specialization, tuning processing to ensure fast and efficient goal attainment. This type of feedback has been suggested in previous theoretical models of visual specialization (Goldstone, 2003), though the suggestion has been anatomically agnostic. Our results hint that the parietal cortex may be the anatomical locus, and this locus varies within the cortex on the basis of the physical constraints of its connectivity. In addition to potential feedback regarding task relevant features, the parietal cortex may also provide architecture for unique computations, such as numerical processing (Knops, Piazza, Sengupta, Eger, & Melcher, 2014; Park, Park, & Polk, 2013), which may also produce unique feedback to shape selectivity.

Recent neuroimaging findings also revealed potential roles of the posterior parietal in shaping visual perception. For example, a recent study examining motion-based scene segregation during a bistable perception task provides an interesting alternative explanation regarding the parietal cortex's role in visual selectivity development. They demonstrated a differential involvement of the AG and SPL, with the AG responding to "default" perceptions of scene segregation, and SPL responding to alternative segregations. Given the current results, an alternative explanation is that the AG's role is in guiding perception of highly learned holistic patterns, as opposed to the SPL which may play a role in segregating more novel patterns (Grassi, Zaretskaya, & Bartels, 2018). While this explanation is somewhat consistent with our results (SPL-Face connectivity predicting less segregated networks), it doesn't fully account for the data (AG-Scene connectivity predicting less segregated networks). However, if it is the case, this provides novel predictions regarding the timecourse of parietal connectivity with the development of visual category specialization. That is, early development should be tracked by relatively stronger functional connectivity from SPL to areas of specialization, while late development should be tracked by stronger functional connectivity from AG to areas of specialization.

It's important to note that our results are also consistent with previous studies examining verbal development. Recent work has demonstrated the importance of the development of parieto-temporal connectivity in the development of normal and abnormal literacy within children of similar ages (Lee, Booth, & Chou, 2016; Morken, Helland, Hugdahl, & Specht, 2017). Given the convergent cross-modality evidence, it seems likely that the development of the parietal functional connectivity is fundamentally important in the general development of sensory association specialization. A more detailed examination of the topology of parietal connectivity across the life span may provide a unifying framework for the development of sensory specialization.

4.2 Biased Connectivity Hypothesis

Our results support the biased connectivity hypothesis as a potential mechanism for cortical specialization (Hannagan et al., 2015). The biased connectivity hypothesis states that extrinsic connectivity patterns constrain a region's intrinsic processing, generating patterns of object selective activity along the inferotemporal cortex. Thus, the development of a region's specialization would be constrained by the time course of development of an extrinsic region (e.g., the posterior parietal cortex) and its connections with the target region, such as the ventral visual pathway areas. This framework provides a mechanism for the differential developmental trajectories of the face and scene processing networks, and provides a potential explanation on why, as the face processing network develops, it's not necessarily the selectivity that increases but the stabilization and expansion of the functional activation in correspondence to task-relevant visual stimuli (Scherf et al., 2007). Indeed, a previous study examining the emergence of the visual word form area had found extrinsic anatomical connectivity to be more predictive of cortical specialization than functional response (Saygin et al., 2016). Indeed, extrinsic anatomical connectivity seems to predict functional specialization in the face and scene processing networks as well, though in adults (Osher et al., 2016). We have extended this work, providing additional evidence for the generalization of the biased connectivity hypothesis to development of cortical specialization of face and scene perception. Further, our work has specified the potential locus of biased connectivity to the parietal cortex, providing a putative explanation for the different developmental trajectories of different cortical specializations.

4.3 Network distance as a measure of visual specialization

Our data support the interpretation of network distance as a measure of network specialization, and extends it to the examinations of small a priori defined networks. Network distance is often shown to represent the specialization of a network, and the degree to which it is integrating information across other networks (Rubinov & Sporns, 2010). Careful attention, however, is required when interpreting different studies examining this metric, as different levels of integration and segregation may co-exist across different tasks and across different networks. Previous studies have found decreases in whole brain network segregation from resting to task state (Di, Gohel, Kim, & Biswal, 2013). Similarly, increasing n-back working memory load leads to decreases in network segregation across whole brain networks (Kitzbichler, Henson, Smith, Nathan, & Bullmore, 2011) and this decrease predicts task performance across load (Stanley, Dagenbach, Lyday, Burdette, & Laurienti, 2014). However, when examining a smaller set of task specific nodes (e.g. fronto-parietal, default mode, and cerebellar networks), increased segregation was shown to positively predict visual short term memory capacity (Stevens, Tappon, Garg, & Fair, 2012). Thus, node selection may play an important role in interpretation of network properties. It is likely for smaller networks with a priori theoretical definitions to demonstrate specialization (through network segregation), while for larger to demonstrate synchronization (through network integration) of goal directed behavior. Indeed, examining a subset of visuo-motor specific nodes it was found that increases in motor learning across a task were associated with increased segregation between these visual and motor modules (Bassett, Yang, Wymbs, & Grafton, 2015).

Changes associated with development, while perhaps often conflated with changes due to learning, may also impact network segregation. Using a data driven machine learning approach, it was found that both network integration and segregation predict brain maturity (Dosenbach et al., 2010). However, network segregation, rather than integration, seems to be more closely linked to brain maturity (Dosenbach et al., 2010). Our findings thus provide empirical evidence for a potential mechanism for the development of network segregation by demonstrating the contribution of extrinsic connectivity.

4.4 Limitations of current work

First and foremost, we must address the lack of a proper adult control group. It isn't possible to tease apart whether the differences we found were due to the population of subjects (children vs adults) or simply a difference between the data itself, as each set was collected with different scanning parameters at different scan sites. However, the main findings of parietal connectivity effects on visual network properties demonstrate internal consistency within the child cohort. Our analysis revealed that parietal connectivity predicted changes in network distance in the direction one would expect from the child and adult comparison. In addition to our adult sample, it's important to note that the age range selected in our child sample has some amount of arbitrariness to it. Optimally, one should study these effects longitudinally across the entire span of development. Without such data, making any claims about developmental effects must be made with hesitance.

The current behavioral task was primarily designed for ROI selection; while it was sufficient for eliciting activity in the face/scene networks, it was not designed to be a full test of face and scene perception. The task is designed to be simple, and thus the behavioral responses do not provide much information about the computations being performed. For this reason, it is unsurprising that the correlations between the fMRI data and the behavioral output were relatively weak. In addition, while it did not impact the main findings of this study, heterogeneity across the different face conditions was evident in both the children's behavior and the extent to which the task drove the face processing network's activation.

A more homogenous stimulus set and a task, such as the inverted face paradigm, that more appropriately assays the specific nature of these processing networks would be needed for future studies to further investigate the relationship between network development and visual perception. The inversion effect, however, is less apparent in the recognition of scenes (Diamond & Carey, 1986). Therefore, it might be better to target the spatial nature of scene processing.

4.5 Conclusion

Despite the limitations, the results from this study provided new insights on the role of posterior parietal connectivity on visual selectivity along the inferotemporal cortex in late childhood or early adolescence. We also highlight the importance of potential parietal development when considering the face and scene processing systems, providing a mechanism for different developmental trajectories for different sensory specializations.

Supplementary Material

Refer to Web version on PubMed Central for supplementary material.

Acknowledgments

We thank Yi Gao for her contributions to this project, primarily within the scope of data quality control. This work was supported by RO1 MH069942 (D. Klein) from the National Institutes of Health and the Stony Brook Research Foundation (H.-C. Leung).

References

Arcaro MJ, Schade PF, Vincent JL, Ponce CR, & Livingstone MS (2017). Seeing faces is necessary for face-domain formation. Nature Neuroscience, 20(10), 1404–1412. 10.1038/nn.4635 [PubMed: 28869581]

Avillac M, Denève S, Olivier E, Pouget A, & Duhamel J-R (2005). Reference frames for representing visual and tactile locations in parietal cortex. Nature Neuroscience, 8(7), 941–949. 10.1038/nn1480 [PubMed: 15951810]

Aylward EH, Park JE, Field KM, Parsons AC, Richards TL, Cramer SC, & Meltzoff AN (2005). Brain activation during face perception: evidence of a developmental change. Journal of Cognitive Neuroscience, 17(2), 308–319. [PubMed: 15811242]

Bassett DS, Yang M, Wymbs NF, & Grafton ST (2015). Learning-induced autonomy of sensorimotor systems. Nature Neuroscience, 18(5), 744–751. 10.1038/nn.3993 [PubMed: 25849989]

Behrmann M, & Plaut DC (2013). Distributed circuits, not circumscribed centers, mediate visual recognition. Trends in Cognitive Sciences, 17(5), 210–219. 10.1016/j.tics.2013.03.007 [PubMed: 23608364]

Biswal BB, Mennes M, Zuo X-N, Gohel S, Kelly C, Smith SM, … Milham MP (2010). Toward discovery science of human brain function. Proceedings of the National Academy of Sciences, 107(10), 4734–4739. 10.1073/pnas.0911855107

Blatt GJ, Andersen RA, & Stoner GR (1990). Visual receptive field organization and cortico-cortical connections of the lateral intraparietal area (area LIP) in the macaque. Journal of Comparative Neurology, 299(4), 421–445. 10.1002/cne.902990404 [PubMed: 2243159]

Buschman TJ, & Miller EK (2007). Top-down versus bottom-up control of attention in the prefrontal and posterior parietal cortices. Science, 315(5820), 1860–1862. [PubMed: 17395832]

Caspers J, Zilles K, Eickhoff SB, Schleicher A, Mohlberg H, & Amunts K (2013). Cytoarchitectonical analysis and probabilistic mapping of two extrastriate areas of the human posterior fusiform gyrus. Brain Structure and Function, 218(2), 511–526. 10.1007/s00429-012-0411-8 [PubMed: 22488096]

Cavada C, & Goldman-Rakic PS (1989). Posterior parietal cortex in rhesus monkey: II. Evidence for segregated corticocortical networks linking sensory and limbic areas with the frontal lobe. The Journal of Comparative Neurology, 287(4), 422–445. 10.1002/cne.902870403 [PubMed: 2477406]

Cohen L, Dehaene S, Naccache L, Lehéricy S, Dehaene-Lambertz G, Hénaff M-A, & Michel F (2000). The visual word form area. Brain, 123(2), 291–307. [PubMed: 10648437]

Culham JC, & Kanwisher NG (2001). Neuroimaging of cognitive functions in human parietal cortex. Current Opinion in Neurobiology, 11(2), 157–163. [PubMed: 11301234]

Deen B, Richardson H, Dilks DD, Takahashi A, Keil B, Wald LL, … Saxe R (2017). Organization of high-level visual cortex in human infants. Nature Communications, 8, 13995 10.1038/ncomms13995

Di X, Gohel S, Kim EH, & Biswal BB (2013). Task vs. rest—different network configurations between the coactivation and the resting-state brain networks. Frontiers in Human Neuroscience, 7 10.3389/fnhum.2013.00493

Diamond R, & Carey S (1986). Why faces are and are not special: an effect of expertise. Journal of Experimental Psychology: General, 115(2), 107. [PubMed: 2940312]

Dosenbach NU, Nardos B, Cohen AL, Fair DA, Power JD, Church JA, … Lessov-Schlaggar CN (2010). Prediction of individual brain maturity using fMRI. Science, 329(5997), 1358–1361. [PubMed: 20829489]

Egly R, Driver J, & Rafal RD (1994). Shifting visual attention between objects and locations: evidence from normal and parietal lesion subjects. Journal of Experimental Psychology: General, 123(2), 161. [PubMed: 8014611]

Epstein R, & Kanwisher N (1998). A cortical representation of the local visual environment. Nature, 392(6676), 598–601. 10.1038/33402 [PubMed: 9560155]

Gogtay N, Giedd JN, Lusk L, Hayashi KM, Greenstein D, Vaituzis AC, … others. (2004). Dynamic mapping of human cortical development during childhood through early adulthood. Proceedings of the National Academy of Sciences of the United States of America, 101(21), 8174–8179. [PubMed: 15148381]

Golarai G, Ghahremani DG, Whitfield-Gabrieli S, Reiss A, Eberhardt JL, Gabrieli JDE, & Grill-Spector K (2007). Differential development of high-level visual cortex correlates with category-specific recognition memory. Nature Neuroscience 10.1038/nn1865

Golarai G, Liberman A, & Grill-Spector K (2017). Experience Shapes the Development of Neural Substrates of Face Processing in Human Ventral Temporal Cortex. Cerebral Cortex, bhv314. 10.1093/cercor/bhv314

Golarai G, Liberman A, Yoon JMD, & Grill-Spector K (2010). Differential development of the ventral visual cortex extends through adolescence. Frontiers in Human Neuroscience 10.3389/neuro.09.080.2009

Goldstone RL (2003). Learning to perceive while perceiving to learn. In Perceptual organization in vision (pp. 245–290). Psychology Press.

Gomez J, Barnett MA, Natu V, Mezer A, Palomero-Gallagher N, Weiner KS, … Grill-Spector K (2017). Microstructural proliferation in human cortex is coupled with the development of face processing. Science, 355(6320), 68–71. 10.1126/science.aag0311 [PubMed: 28059764]

Gomez J, Pestilli F, Witthoft N, Golarai G, Liberman A, Poltoratski S, … Grill-Spector K (2015). Functionally Defined White Matter Reveals Segregated Pathways in Human Ventral Temporal Cortex Associated with Category-Specific Processing. Neuron, 85(1), 216–227. 10.1016/j.neuron.2014.12.027 [PubMed: 25569351]

Grassi PR, Zaretskaya N, & Bartels A (2018). A generic mechanism for perceptual organization in the parietal cortex. The Journal of Neuroscience, 0436–18. 10.1523/JNEUROSCI.0436-18.2018

Grill-Spector K, Weiner KS, Kay K, & Gomez J (2017). The Functional Neuroanatomy of Human Face Perception. Annual Review of Vision Science, 3(1), 167–196. 10.1146/annurev-vision-102016-061214

Hannagan T, Amedi A, Cohen L, Dehaene-Lambertz G, & Dehaene S (2015). Origins of the specialization for letters and numbers in ventral occipitotemporal cortex. Trends in Cognitive Sciences, 19(7), 374–382. [PubMed: 26072689]

Helbig HB, Graf M, & Kiefer M (2006). The role of action representations in visual object recognition. Experimental Brain Research, 174(2), 221–228. 10.1007/s00221-006-0443-5 [PubMed: 16636796]

Husain M, & Nachev P (2007). Space and the parietal cortex. Trends in Cognitive Sciences, 11(1), 30–36. 10.1016/j.tics.2006.10.011 [PubMed: 17134935]

Janssen P, Srivastava S, Ombelet S, & Orban GA (2008). Coding of Shape and Position in Macaque Lateral Intraparietal Area. Journal of Neuroscience, 28(26), 6679–6690. 10.1523/JNEUROSCI.0499-08.2008 [PubMed: 18579742]

Johnson MH (2011). Interactive Specialization: A domain-general framework for human functional brain development? Developmental Cognitive Neuroscience, 1(1), 7–21. 10.1016/j.dcn.2010.07.003 [PubMed: 22436416]

Kann SJ, O'Rawe JF, Huang AS, Klein DN, & Leung H-C (2017). Preschool negative emotionality predicts activity and connectivity of the fusiform face area and amygdala in later childhood. Social Cognitive and Affective Neuroscience, 12(9), 1511–1519. 10.1093/scan/nsx079 [PubMed: 28992271]

Kanwisher N, McDermott J, & Chun MM (1997). The fusiform face area: a module in human extrastriate cortex specialized for face perception. The Journal of Neuroscience, 17(11), 4302–4311. [PubMed: 9151747]

Kay KN, Weiner KS, & Grill-Spector K (2015). Attention Reduces Spatial Uncertainty in Human Ventral Temporal Cortex. Current Biology, 25(5), 595–600. 10.1016/j.cub.2014.12.050 [PubMed: 25702580]

Kay KN, & Yeatman JD (2017). Bottom-up and top-down computations in word-and face-selective cortex. Elife, 6, e22341. [PubMed: 28226243]

Kitzbichler MG, Henson RNA, Smith ML, Nathan PJ, & Bullmore ET (2011). Cognitive Effort Drives Workspace Configuration of Human Brain Functional Networks. Journal of Neuroscience, 31(22), 8259–8270. 10.1523/JNEUROSCI.0440-11.2011 [PubMed: 21632947]

Knops A, Piazza M, Sengupta R, Eger E, & Melcher D (2014). A Shared, Flexible Neural Map Architecture Reflects Capacity Limits in Both Visual Short-Term Memory and Enumeration. Journal of Neuroscience, 34(30), 9857–9866. 10.1523/JNEUROSCI.2758-13.2014 [PubMed: 25057189]

Konen CS, & Kastner S (2008). Two hierarchically organized neural systems for object information in human visual cortex. Nature Neuroscience, 11(2), 224–231. 10.1038/nn2036 [PubMed: 18193041]

Kravitz DJ, Saleem KS, Baker CI, & Mishkin M (2011). A new neural framework for visuospatial processing. Nature Reviews Neuroscience, 12(4), 217–230. 10.1038/nrn3008 [PubMed: 21415848]

Kravitz DJ, Saleem KS, Baker CI, Ungerleider LG, & Mishkin M (2013). The ventral visual pathway: an expanded neural framework for the processing of object quality. Trends in Cognitive Sciences, 17(1), 26–49. 10.1016/j.tics.2012.10.011 [PubMed: 23265839]

Kriegeskorte N, Mur M, Ruff DA, Kiani R, Bodurka J, Esteky H, … Bandettini PA (2008). Matching Categorical Object Representations in Inferior Temporal Cortex of Man and Monkey. Neuron, 60(6), 1126–1141. 10.1016/j.neuron.2008.10.043 [PubMed: 19109916]

Lee S-H, Booth JR, & Chou T-L (2016). Temporo-parietal connectivity uniquely predicts reading change from childhood to adolescence. NeuroImage, 142, 126–134. 10.1016/j.neuroimage.2016.06.055 [PubMed: 27377221]

Lorenz S, Weiner KS, Caspers J, Mohlberg H, Schleicher A, Bludau S, … Amunts K (2017). Two New Cytoarchitectonic Areas on the Human Mid-Fusiform Gyrus. Cerebral Cortex, 27(1), 373–385. 10.1093/cercor/bhv225 [PubMed: 26464475]

Mahon BZ, Anzellotti S, Schwarzbach J, Zampini M, & Caramazza A (2009). Category-Specific Organization in the Human Brain Does Not Require Visual Experience. Neuron, 63(3), 397–405. 10.1016/j.neuron.2009.07.012 [PubMed: 19679078]

Mahon BZ, & Caramazza A (2011). What drives the organization of object knowledge in the brain? Trends in Cognitive Sciences, 15(3), 97–103. 10.1016/j.tics.2011.01.004 [PubMed: 21317022]

Malach R, Levy I, & Hasson U (2002). The topography of high-order human object areas. Trends in Cognitive Sciences, 6(4), 176–184. [PubMed: 11912041]

McGugin RW, Van Gulick AE, & Gauthier I (2016). Cortical Thickness in Fusiform Face Area Predicts Face and Object Recognition Performance. Journal of Cognitive Neuroscience, 28(2), 282–294. 10.1162/jocn_a_00891 [PubMed: 26439272]

Mishkin M, & Ungerleider LG (1982). Contribution of striate inputs to the visuospatial functions of parieto-preoccipital cortex in monkeys. Behavioural Brain Research, 6(1), 57–77. [PubMed: 7126325]

Morken F, Helland T, Hugdahl K, & Specht K (2017). Reading in dyslexia across literacy development: A longitudinal study of effective connectivity. NeuroImage, 144, 92–100. 10.1016/j.neuroimage.2016.09.060 [PubMed: 27688204]

Murphy K, Birn RM, Handwerker DA, Jones TB, & Bandettini PA (2009). The impact of global signal regression on resting state correlations: Are anti-correlated networks introduced? NeuroImage, 44(3), 893–905. 10.1016/j.neuroimage.2008.09.036 [PubMed: 18976716]

Olino TM, Klein DN, Dyson MW, Rose SA, & Durbin CE (2010). Temperamental emotionality in preschool-aged children and depressive disorders in parents: Associations in a large community

sample. Journal of Abnormal Psychology, 119(3), 468–478. 10.1037/a0020112 [PubMed: 20677836]

Orban GA (2016). Functional definitions of parietal areas in human and non-human primates. Proceedings of the Royal Society B: Biological Sciences, 283(1828), 20160118 10.1098/rspb.2016.0118

Orban GA, Van Essen D, & Vanduffel W (2004). Comparative mapping of higher visual areas in monkeys and humans. Trends in Cognitive Sciences, 8(7), 315–324. 10.1016/j.tics.2004.05.009 [PubMed: 15242691]

Osher DE, Saxe RR, Koldewyn K, Gabrieli JDE, Kanwisher N, & Saygin ZM (2016). Structural Connectivity Fingerprints Predict Cortical Selectivity for Multiple Visual Categories across Cortex. Cerebral Cortex, 26(4), 1668–1683. 10.1093/cercor/bhu303 [PubMed: 25628345]

Palmeri TJ, Wong AC-N, & Gauthier I (2004). Computational approaches to the development of perceptual expertise. Trends in Cognitive Sciences, 8(8), 378–386. 10.1016/j.tics.2004.06.001 [PubMed: 15335465]

Park J, Park DC, & Polk TA (2013). Parietal Functional Connectivity in Numerical Cognition. Cerebral Cortex, 23(9), 2127–2135. 10.1093/cercor/bhs193 [PubMed: 22784605]

Proklova D, Kaiser D, & Peelen MV (2016). Disentangling Representations of Object Shape and Object Category in Human Visual Cortex: The Animate–Inanimate Distinction. Journal of Cognitive Neuroscience, 28(5), 680–692. 10.1162/jocn_a_00924 [PubMed: 26765944]

Rubinov M, & Sporns O (2010). Complex network measures of brain connectivity: Uses and interpretations. NeuroImage, 52(3), 1059–1069. 10.1016/j.neuroimage.2009.10.003 [PubMed: 19819337]

Rushworth MFS, Behrens TEJ, & Johansen-Berg H (2006). Connection Patterns Distinguish 3 Regions of Human Parietal Cortex. Cerebral Cortex, 16(10), 1418–1430. 10.1093/cercor/bhj079 [PubMed: 16306320]

Sarma A, Masse NY, Wang X-J, & Freedman DJ (2015). Task-specific versus generalized mnemonic representations in parietal and prefrontal cortices. Nature Neuroscience, 19(1), 143–149. 10.1038/nn.4168 [PubMed: 26595652]

Sarma A, Masse NY, Wang X-J, & Freedman DJ (2016). Task-specific versus generalized mnemonic representations in parietal and prefrontal cortices. Nature Neuroscience, 19(1), 143–149. 10.1038/nn.4168 [PubMed: 26595652]

Saygin ZM, Osher DE, Norton ES, Youssoufian DA, Beach SD, Feather J, … Kanwisher N (2016). Connectivity precedes function in the development of the visual word form area. Nature Neuroscience, 19(9), 1250–1255. 10.1038/nn.4354 [PubMed: 27500407]

Scherf KS, Behrmann M, Humphreys K, & Luna B (2007). Visual category-selectivity for faces, places and objects emerges along different developmental trajectories. Developmental Science, 10(4), F15–F30. 10.1111/j.1467-7687.2007.00595.x [PubMed: 17552930]

Schmahmann JD, & Pandya DN (1990). Anatomical investigation of projections from thalamus to posterior parietal cortex in the rhesus monkey: a WGA-HRP and fluorescent tracer study. Journal of Comparative Neurology, 295(2), 299–326. [PubMed: 1694186]

Seltzer B, & Pandya D (1984). Further observations on parieto-temporal connections in the rhesus monkey. Experimental Brain Research, 55(2), 301–312. [PubMed: 6745368]

Sereno AB, & Maunsell JHR (1998). Shape selectivity in primate lateral intraparietal cortex. Nature, 395(6701), 500–503. 10.1038/26752 [PubMed: 9774105]

Shmuelof L, & Zohary E (2005). Dissociation between Ventral and Dorsal fMRI Activation during Object and Action Recognition. Neuron, 47(3), 457–470. 10.1016/j.neuron.2005.06.034 [PubMed: 16055068]

Shum J, Hermes D, Foster BL, Dastjerdi M, Rangarajan V, Winawer J, … Parvizi J (2013). A Brain Area for Visual Numerals. Journal of Neuroscience, 33(16), 6709–6715. 10.1523/JNEUROSCI.4558-12.2013 [PubMed: 23595729]

Silver MA (2005). Topographic Maps of Visual Spatial Attention in Human Parietal Cortex. Journal of Neurophysiology, 94(2), 1358–1371. 10.1152/jn.01316.2004 [PubMed: 15817643]

Singh-Curry V, & Husain M (2009). The functional role of the inferior parietal lobe in the dorsal and ventral stream dichotomy. Neuropsychologia, 47(6), 1434–1448. 10.1016/j.neuropsychologia.2008.11.033 [PubMed: 19138694]

Stanley ML, Dagenbach D, Lyday RG, Burdette JH, & Laurienti PJ (2014). Changes in global and regional modularity associated with increasing working memory load. Frontiers in Human Neuroscience, 8 10.3389/fnhum.2014.00954

Stevens AA, Tappon SC, Garg A, & Fair DA (2012). Functional Brain Network Modularity Captures Inter- and Intra-Individual Variation in Working Memory Capacity. PLoS ONE, 7(1), e30468 10.1371/journal.pone.0030468 [PubMed: 22276205]

Swaminathan SK, & Freedman DJ (2012). Preferential encoding of visual categories in parietal cortex compared with prefrontal cortex. Nature Neuroscience, 15(2), 315–320. 10.1038/nn.3016 [PubMed: 22246435]

Taylor MJ, Batty M, & Itier RJ (2004). The faces of development: a review of early face processing over childhood. Journal of Cognitive Neuroscience, 16(8), 1426–1442. [PubMed: 15509388]

Tzourio-Mazoyer N, Landeau B, Papathanassiou D, Crivello F, Etard O, Delcroix N, … Joliot M (2002). Automated Anatomical Labeling of Activations in SPM Using a Macroscopic Anatomical Parcellation of the MNI MRI Single-Subject Brain. NeuroImage, 15(1), 273–289. 10.1006/nimg.2001.0978 [PubMed: 11771995]

Van Essen DC, & Gallant JL (1994). Neural mechanisms of form and motion processing in the primate visual system. Neuron, 13(1), 1–10. [PubMed: 8043270]

Von Der Heide RJ, Skipper LM, & Olson IR (2013). Anterior temporal face patches: a meta-analysis and empirical study. Frontiers in Human Neuroscience, 7 10.3389/fnhum.2013.00017

Vuilleumier P, Henson RN, Driver J, & Dolan RJ (2002). Multiple levels of visual object constancy revealed by event-related fMRI of repetition priming. Nature Neuroscience, 5(5), 491–499. 10.1038/nn839 [PubMed: 11967545]

Weiner KS, Barnett MA, Lorenz S, Caspers J, Stigliani A, Amunts K, … Grill-Spector K (2017). The Cytoarchitecture of Domain-specific Regions in Human High-level Visual Cortex. Cerebral Cortex, 27(1), 146–161. 10.1093/cercor/bhw361 [PubMed: 27909003]

Xing J, & Andersen RA (2000). Models of the posterior parietal cortex which perform multimodal integration and represent space in several coordinate frames. Journal of Cognitive Neuroscience, 12(4), 601–614. [PubMed: 10936913]

Yarkoni T, Poldrack RA, Nichols TE, Van Essen DC, & Wager TD (2011). Large-scale automated synthesis of human functional neuroimaging data. Nature Methods, 8(8), 665–670. 10.1038/nmeth.1635 [PubMed: 21706013]

- Children's face and scene processing networks are less segregated
- These networks are influenced by different parts of the posterior parietal cortex
- Functional connectivity from posterior parietal cortex predicts network segregation
- Spatial patterns of posterior parietal cortex connectivity predict rFFA location

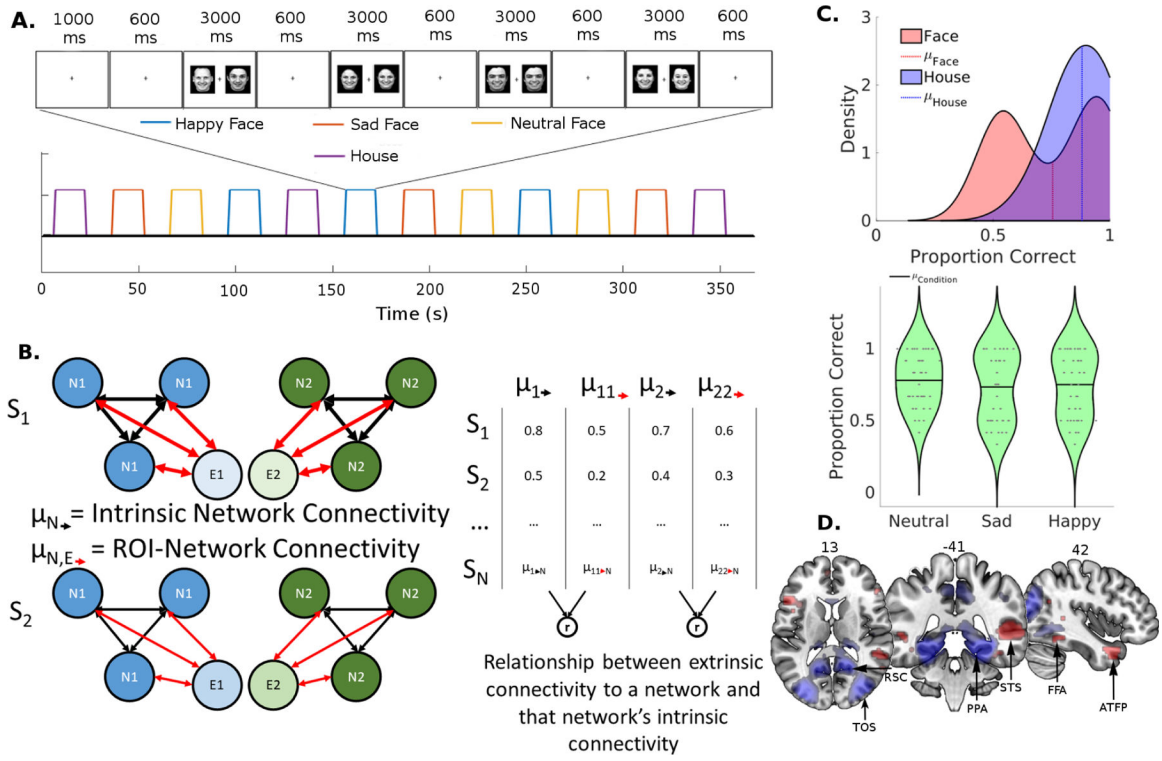

Figure 1:

(A) Stimulus Identity Matching Task. One of two counterbalances is shown in the form of a boxcar functions. As an example, the 6th block is expanded to demonstrate the sequence of visual stimulus presentation within the block. Subjects made button presses to indicate whether or not each pair of visual stimuli matched in identity. **(B)** Schematic of the resting state functional connectivity metrics. The left depicts two hypothetical subjects, and the diagrams illustrate the relationship between two networks (N1/N2, e.g. face and scene networks) and two extrinsic ROIs (E1/E2, e.g. AG and SPL). Intrinsic connectivity strength is calculated as the average of the black arrows within each visual network, while ROI-Network connectivity (extrinsic connectivity) is calculated as an average of the red arrows from one external ROI to each node in a network. The correlation between these two metrics (right) is used to estimate the extent to which a the network-like behavior of a set of nodes in a visual network would depend on extrinsic connectivity. **(C)** *Top:* Distributions of performance accuracy on face and scene conditions in children as estimated by Kernal Density Estimation. *Bottom:* Violin Plots demonstrating the variance in performance accuracy for the face conditions. Each data point is plotted within the distribution, data points were randomly jittered along the x-axis for visualization. **(D)** Face > House (Red) and House > Face (Blue) group contrasts overlaid on an MNI template brain thresholded at $p < .001$. ROIs in the face processing network: fusiform face area (FFA), superior temporal sulcus (STS), and anterior temporal face patch (ATFP). ROIs in the scene network: parahippocampal place area (PPA), retrosplenial cortex (RSC), and transverse occipital sulcus (TOS).

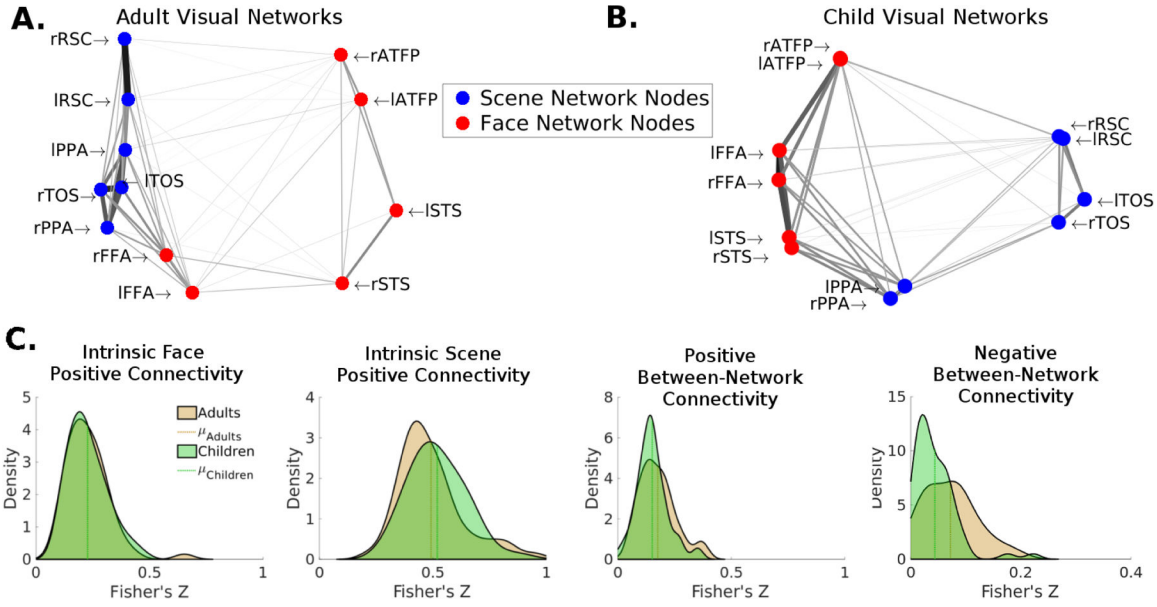

Figure 2:

Intrinsic functional connectivity of the face and scene networks during resting state fMRI. **(A)** Face and scene networks in the adult sample. **(B)** Face and scene networks in the child sample. For both A & B a distance matrix was calculated as 1-**R** and multidimensional scaling was performed to produce two arbitrary dimensions that maintain the bivariate distances between each set of nodes. The darkness and thickness of the edges connecting any two nodes is scaled by the correlation between those two nodes, such that darker thicker edges represent stronger correlations (edges only represent positive correlations). **(C)** Distributions of within-network (intrinsic), and between-network connectivity strength of the face and scene networks in the child sample relative to the adult sample. The children showed weaker segregation between the face and scene networks, as shown by their relatively lower negative between-network connectivity.

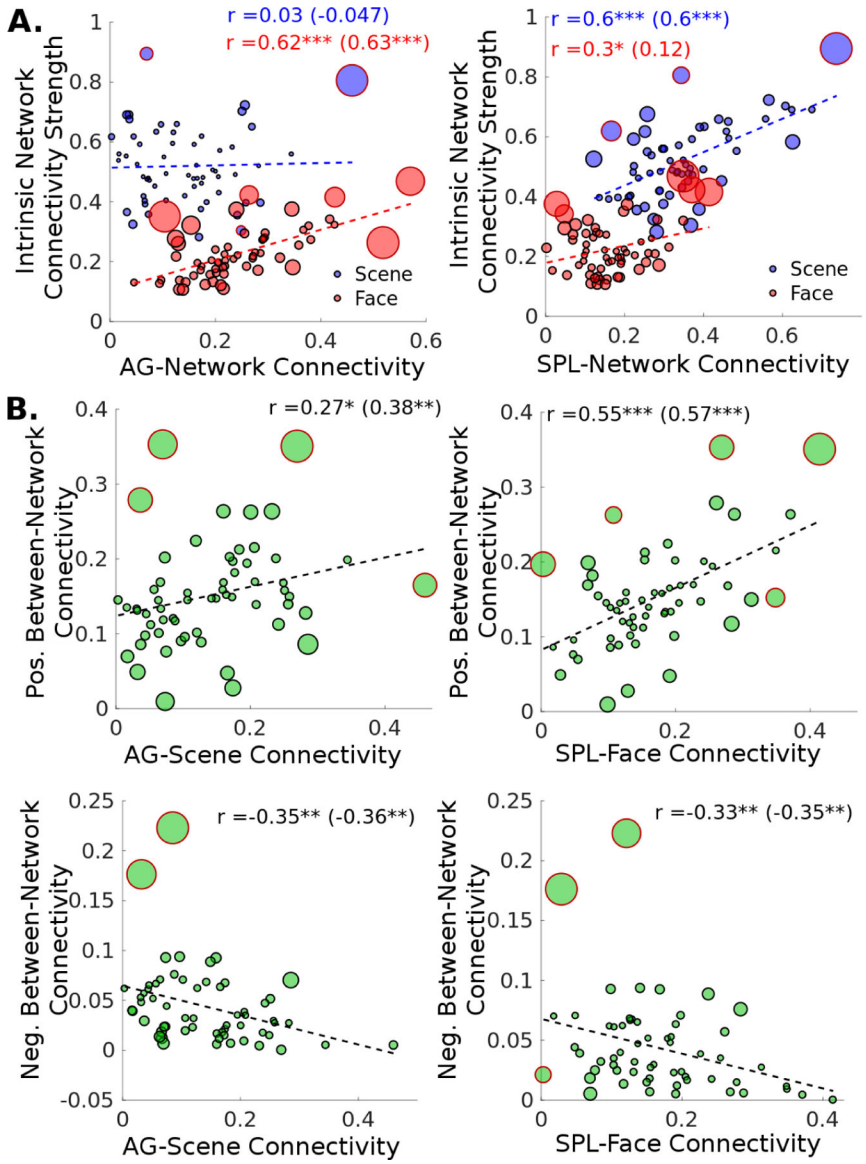

Figure 3:

Children's posterior parietal functional connectivity with the face and scene networks during resting state fMRI (N = 60). **(A)** The degree of connectivity between parietal regions and the face and scene networks have differential effects on the visual network's intrinsic connectivity strength. (AG, angular gyrus; SPL, superior parietal lobule) **(B)** AG/SPL connectivity with non-preferred visual network is associated with weaker segregation between face and scene networks (i.e. lower negative and higher positive between-network connectivity). In all scatter plots, each datapoint's size is scaled linearly with the point's Cook's d, a measure of influence, and the datapoints with red outlines rather than black are outliers as classifed by the rule of thumb Cook's d > n/4. The bivariate correlations are shown, and the correlations with outliers excluded in parentheses.

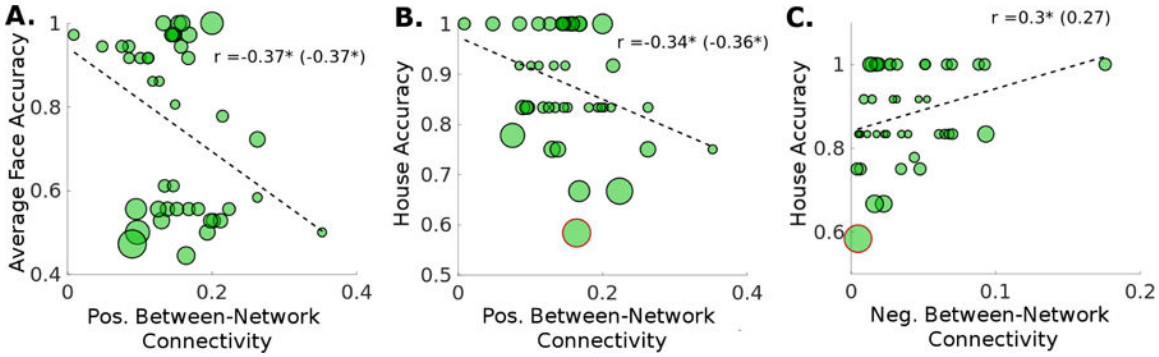

Figure 4:

Relationship between network distance and task performance in a subset of children with performance data (N = 43). Greater positive between network connectivity (i.e. weaker segregation between the face and scene networks) was associated with poorer performance on the face condition **(A)** and the scene condition **(B)**, while greater negative between network connectivity (i.e. stronger segregation between the visual networks) was associated with better house performance **(C)**.

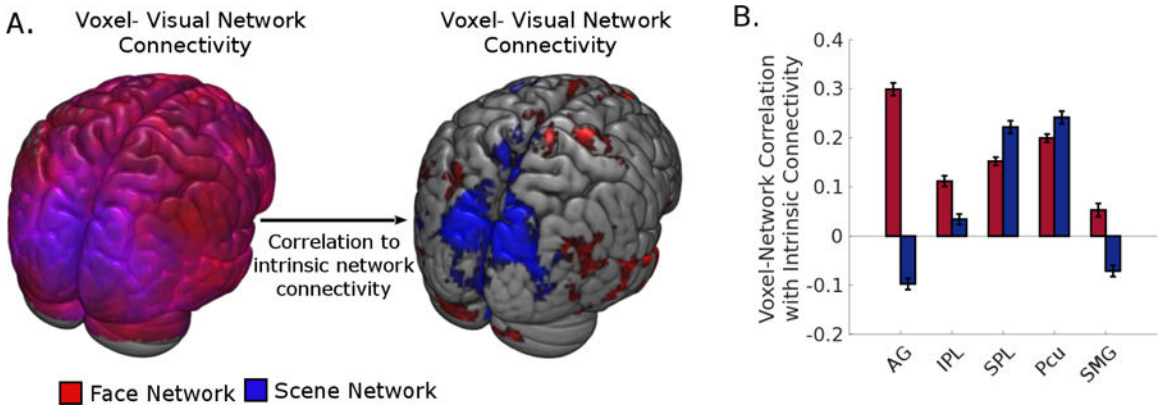

Figure 5:

A voxel-wise analysis of the relationship between extrinsic connecitivty effect and visual networks' intrinsic connectivity. **(A) Left:** Each voxel represents average connctivity strength between that voxel and each node within the face and scene networks, thresholded at $p < .001$. **Right:** Each voxel represents the level of association between a voxel's average connectivity with the face/scene network and the corresponding visual network's intrinsic network connectivity strength, thresholded at $p < .001$. **(B)** Quantification of the level of association between parietal regions and the two visual networks' intrinsic connectivity strength. Error bars represent 95% confidence intervals. Abbreviations: AG, angular gyrus; IPL, inferior parietal lobule; SPL, superior parietal lobule; Pcu, precuneus; SMG, supramarginal gyrus.

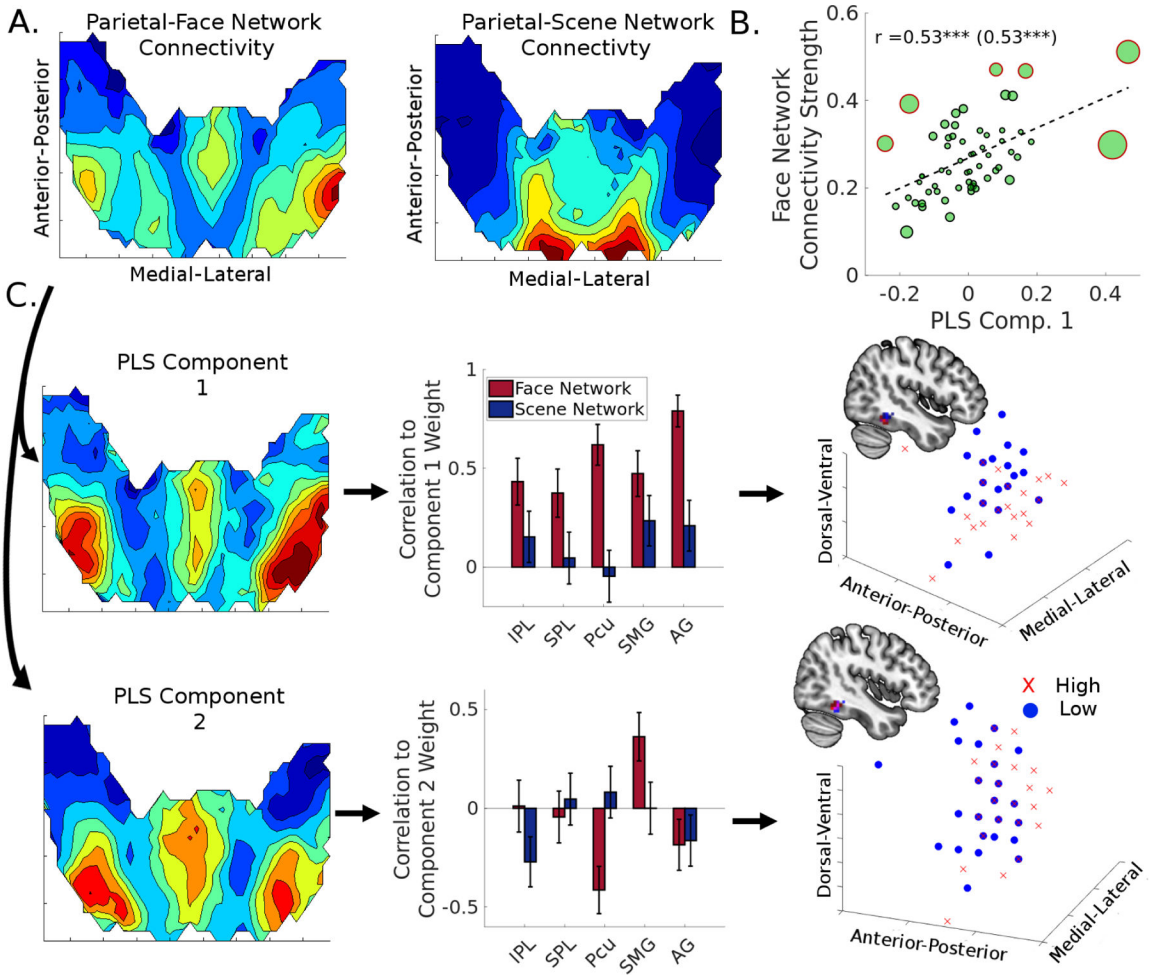

Figure 6:

Partial Least Squares (PLS) regression demonstrates that the variation in location of the right fusiform face area (rFFA) across children depends on the spatial pattern of its connectivity with the parietal lobe. **(A)** Parietal-face and parietal-scene network connectivity patterns, collapsed across the dorsal-ventral axis of the posterior parietal cortex. **(B)** Higher component score for PLS Component 1 was associated with stronger intrinsic connectivity within the face network. **(C)** Characterization of the PLS regression analysis for the parietal-face network connectivity. The first two components account for 31.26% of the variance in rFFA location, with Component 1 (AG-component) yielding a posterior and ventral shift, and Component 2 (SMG-component) yielding a posterior shift. The three dimensional scatter plots represent the centroids of each subject's rFFA, with red X's representing participants with a higher weight and blue circles representing particiapnts with a lower weight for each component.

Table 1:

Peak coordinates for functionally localized face and scene ROIs in MNI space. Abbreviations: FFA: Fusiform Face Area, STS: Superior Temporal Sulcus, ATFP: Anterior Temporal Face Patch, PPA: Parahippocampal Place Area, TOS: Transverse Occipital Sulcus, RSC: Retrosplenial Cortex

Region	*MNI Coordinates*			Peak t-value
	X	Y	Z	
lFFA	−42	−45	−15	4.28
rFFA	42	−45	6	5.42
lSTS	−48	−36	−3	3.65
rSTS	60	−42	6	4.83
lATFP	−42	15	−30	3.74
rATFP	42	12	−30	5.50
lPPA	−27	−48	−6	26.18
rPPA	30	−48	−6	26.81
lTOS	−30	−84	24	17.63
rTOS	36	−81	24	16.41
lRSC	−18	−60	18	12.60
rRSC	18	−54	21	15.89

Table 2:

Results from multiple regression analysis of network distance in association with parietal-visual network connectivity. Unstandardized b-weights are shown, with standard errors in parentheses.

	Between Network Positive Connectivity:	**Between Network Negative Connectivity:**
SPL-Face Connectivity	0.327*** (0.094)	−0.148* (0.058)
SPL-Scene Connectivity	0.107 (0.060)	0.033 (0.037)
AG-Face Connectivity	−0.026 (0.072)	0.096* (0.044)
AG-Scene Connectivity	0.123 (0.083)	−0.122* (0.051)
Constant	0.049 (0.028)	0.051** (0.018)
N	60	60
R^2	0.357	0.256
Adjusted R^2	0.310	0.201
F (4, 55)	7.63***	4.72**

* p<0.05

** p<0.01

*** p<0.001